Inorg. Chem. **2002**, *41*, 973–980

Solid-State Structures of Zinc(II) Benzoate Complexes. Catalyst Precursors for the Coupling of Carbon Dioxide and Epoxides

Donald J. Darensbourg,* Jacob R. Wildeson, and Jason C. Yarbrough

Department of Chemistry, Texas A&M University, P.O. Box 30012, College Station, Texas 77842

Received July 27, 2001

Zinc complexes derived from benzoic acids containing electron-withdrawing substituents have been synthesized from Zn^{II}(bis-trimethylsilyl amide)$_2$ and the corresponding carboxylic acid (2,6-$X_2C_6H_3COOH$, where X = F, Cl, or OMe) in THF and structurally characterized via X-ray crystallography. The 2,6-difluorobenzoate complex crystallizes from THF or CH_3CN as a seven membered zinc aggregate, where the metal atoms are interconnected by a combination of 10 μ-benzoates and μ_4-oxo ligands, that is, [(2,6-difluorobenzoate)$_{10}O_2Zn_7$](solvent)$_2$, solvent = THF (**1**) and CH_3CN (**1a**). On the other hand, the 2,6-dichlorobenzoate zinc derivative crystallizes from THF as a dimer, [(2,6-dichlorobenzoate)$_4Zn_2$](THF)$_3$ (**2**), where the two zinc centers are bridged by three benzoate ligand. One of the zinc centers possesses a tetrahedral ligand environment where the fourth ligand is a unidentate benzoate, and the other zinc center has an octahedral arrangement of ligands which is accomplished by the additional binding of three THF molecules. Upon dissolution of complex **1** or **2** in the strongly binding pyridine solvent, disruption of these zinc carboxylates occurs with concomitant formation of mononuclear zinc bis-benzoates with three pyridine ligands in the metal coordination sphere. Complexes **1** and **2** were found to be effective catalysts for the copolymerization of cyclohexene oxide and carbon dioxide to afford polycarbonates devoid of polyether linkages, that is, completely alternating copolymers. Although these catalysts or catalyst precursors in the presence of CO_2/propylene oxide afforded mostly propylene carbonate, they did serve as efficient catalysts for the terpolymerization of carbon dioxide/cyclohexene oxide/propylene oxide. The reactivities of these zinc carboxylates were very similar to those previously reported analogous complexes which have not been structurally characterized. Hence, it is suggested here that all of these zinc carboxylates provide similar catalytic sites for CO_2/epoxide coupling processes.

Introduction

During the 1970s, many heterogeneous multicentered zinc catalysts were reported for the coupling of epoxides and carbon dioxide. Prominent among these catalysts were zinc derivatives of mono- and dicarboxylic acids.[1,2] More recently, a methylene chloride soluble zinc complex derived from the monoester of maleic acid has been developed by ARCO for the copolymerization of carbon dioxide and epoxides.[3] The catalytic activity of this system was further enhanced upon fluorination of the ester group by Super et al.[4] which provided solubility of the catalyst in carbon dioxide. In addition, we have reported a comparably active catalyst in the form of a soluble zinc crotonate precursor.[5] In all of these instances, the catalyst structures were not specifically defined because of the inability to isolate single crystals of these zinc carboxylates.

To better identify reaction pathways in this rather complex catalytic process, it is essential to have well-defined structures of the initial metal species employed as catalysts. This is of particular consequence because formation of the generally undesirable cyclic carbonates is the dominant pathway in these soluble catalytic systems when employing *aliphatic* epoxides as monomers. This is in contrast to what is observed in the heterogeneous systems of Inoue[1] and Soga.[2] Formation of cyclic carbonates is attributed to a back biting mechanism

* Author to whom correspondence should be addressed. E-mail: DJDarens@mail.chem.tamu.edu.

(1) Inoue, S.; Kobayashi, M.; Tsuruta, T. *J. Polym. Sci.* **1973**, *11*, 2383.
(2) Soga, K.; Imai, E.; Hattori, I. *Polymer* **1981**, *13* (4), 407.
(3) Sun, H.-N. (Arco Chemical Co.) U.S. Patent 4,783, 445, Nov 8, 1988.
(4) Super, M.; Berluche, E.; Costello, C.; Beckman, E. *Macromolecules* **1997**, *30*, 368.
(5) Darensbourg, D. J.; Zimmer, M. S. *Macromolecules* **1999**, *32*, 2137.

10.1021/ic0107983 CCC: $22.00
Published on Web 02/01/2002

Scheme 1

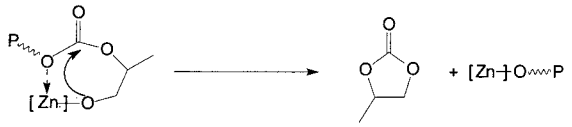

in which a propagating polymer chain coordinates itself to an open zinc center (see Scheme 1). Kuran has suggested the activity of Inoue's catalysts for the copolymerization of propylene oxide is due to an aggregated multicentered zinc system in which a neighboring zinc prevents a propagating polymer chain from back biting on itself.[6] In general, this back biting process responsible for cyclic carbonate production is not an important side reaction in the copolymerization of *alicyclic* epoxides, for example, cyclohexene oxide, with carbon dioxide. Indeed, several homogeneous catalysts have been quite effective for the copolymerization of cyclohexene oxide and carbon dioxide to produce high molecular weight polycarbonates with little to no cyclic carbonate product.[7−11] Although the design of these latter catalyst systems has focused on providing steric environments around the zinc center blocking polymer chain "back biting" processes, none have been reported to be very successful for the copolymerization of aliphatic epoxides, such as propylene oxide, with CO_2.

Herein, we describe the synthesis and characterization of soluble multicentered zinc benzoate clusters utilizing halogenated ligands, which coordinate to the zinc centers in a unidentate, chelating, or bridging fashion. These catalysts display the ability to copolymerize cyclohexene oxide and CO_2 and terpolymerize cyclohexene oxide and propylene oxide with CO_2. In addition, these catalysts do not lose their activity when allowed to stand in air similar to previous zinc phenoxide catalyst systems with halogenated substituents.[12]

Experimental Section

Methods and Materials. Unless otherwise specified, all syntheses and manipulations were carried out on a double manifold Schlenk vacuum line under an atmosphere of argon or in an argon filled glovebox. Glassware was flame dried thoroughly prior to use. Solvents were freshly distilled from sodium benzophenone before use. Cyclohexene oxide and propylene oxide were purchased from Aldrich Chemical Co. and purified by distillation over calcium hydride. Bone dry carbon dioxide was purchased from Scott Specialty Gases, Inc. 2,6-Difluorobenzoic acid, 2,6-dichlorobenzoic acid, and 2,6-dimethoxybenzoic acid were purchased from Lancaster Chemical Co. and were sublimed and stored in a glovebox prior to use. $Zn[N(SiMe_3)_2]_2$ was prepared according to published literature,[13] stored in the glovebox, and used immediately after removal from the box. Infrared spectra were recorded on a Mattson 6081 spectrometer with DTGS and mercury cadmium telluride (MCT) detectors. All isotopically labeled solvents for NMR experiments were purchased from Cambridge Isotope Laboratories. ^1H and ^{13}C NMR spectra were recorded on Varian XL-200E, Unity +300 MHz, and VXR 300 MHz superconducting high-resolution spectrometers. ^{19}F data were acquired on a Unity +300 MHz superconducting NMR spectrometer operating at 282 MHz and referenced to 10% $CFCl_3$ and 1% $CClH_2CClF_2$ in d_6-acetone. Elemental analyses were carried out by Galbraith Laboratories Inc.

Synthesis of $[(2,6\text{-Difluorobenzoate})_{10}O_2Zn_7](THF)_2$ (1). A 5-mL THF solution of 2,6-difluorobenzoic acid (0.164 g, 1.04 mmol) was added to a 5-mL THF solution of $Zn[N(SiMe_3)_2]_2$ (0.20 g, 0.52 mmol), leading to a clear, colorless solution which was stirred at room temperature for 2 h. The solution was then concentrated to 5 mL and stored at −20 °C. Colorless block crystals formed after several days. The supernatant was cannulated off, and crystals were dried under vacuum and collected to yield 0.130 g of product (77%). Anal. Calcd. for $C_{78}H_{46}O_{24}F_{20}Zn_7$ according to the crystal structure: C, 42.49; H, 2.11. Found: C, 43.07; H, 1.91. IR(ν_{CO_2}): (KBr) 1620(s), 1604(s) 1561(s), 1416(br) cm^{-1}; (THF) 1623(s), 1592(m), 1411(s) cm^{-1}. ^1H NMR (CD_3CN): δ 1.78 [m, 8H {THF}], 3.65 [m, 8H {THF}], 6.99 [m, 10H {4-H}], 7.42 [t, 20H {3,5-H}]. $^{13}C\{H\}$ NMR (CD_3CN): δ 26.62 {THF}, 68.73 {THF}, 112.92−113.43 [m, {3,5-C_6H_3} {4-C_6H_3}], 132.83 [t, J_{C-F} = 10.1 Hz {ipso-C_6H_3}], 161.11 [dd, J_{C-Fl} = 250.79 Hz, J_{C-F2} = 8.05 Hz {2,6-C_6H_3}], 169.97 [s, {$-CO_2$}]. $^{19}F\{H\}$ NMR (CD_3CN): δ −112.34.

Synthesis of $[(2,6\text{-Dichlorobenzoate})_4Zn_2](THF)_3$ (2). A 10-mL THF solution of 2,6-dichlorobenzoic acid (0.200 g, 1.04 mmol) was added to a 5-mL THF solution of $Zn[N(SiMe_3)_2]_2$ (0.20 g, 0.52 mmol), leading to a clear, colorless solution which was stirred at room temperature for 2 h. The solution was then concentrated to 5 mL and stored at −20 °C. Colorless block crystals formed after several days. The supernatant was cannulated off, and crystals were dried under vacuum and collected to yield 0.161 g of product (56%). Anal. Calcd. for $C_{40}H_{36}O_{11}Cl_8Zn_2$ according to the crystal structure: C, 43.39; H, 3.28. Anal. Calcd. for $C_{28}H_{12}O_8Cl_8Zn_2$ without bound THF molecules: C, 37.75; H, 1.36. Found: C, 38.16; H, 1.86. A better match between the calculated values for **2** which contained no bound THF molecules was found. This is due to the lability of THF molecules. ^1H NMR also supports this conclusion by exhibiting only trace amounts of THF once the solvent is removed under vacuum. IR(ν_{CO_2}): (KBr) 1610(m), 1591(s), 1556(s), 1404(s) cm^{-1}; (THF) 1626(s), 1589(m), 1399(m) cm^{-1}. ^1H NMR (CD_3CN): δ 1.78 [m, 4H {THF}], 3.74 [m, 4H {THF}], 6.45 [m, 4H], 6.90 [t, 8H, {3,5-H}]. $^{13}C\{H\}$ NMR (CD_3CN): δ 26.62 {THF}, 68.73 {THF}, 129.28, 129.59 [s, {4-C_6H_3}]; 131.09, 131.51

(6) Rokicki, A.; Kuran, W. *J. Macromol. Sci., Rev, Macromol. Chem. Phys.* **1981**, *C21*, 135.
(7) (a) Cheng, M.; Lobkovsky, E.; Coates, G. *J. Am. Chem. Soc.* **1998**, *120*, 11018. (b) Cheng, M.; Moore, D. R.; Reczek, J. J.; Chamberlain, B. M.; Lobkovsky, E. B.; Coates, G. W. *J. Am. Chem. Soc.* **2001**, *123*, 8738.
(8) (a) Darensbourg, D. J.; Zimmer, M.; Rainey, P.; Larkins, D. L. *Inorg. Chem.* **2000**, *39*, 1578. (b) Darensbourg, D. J.; Zimmer, M.; Rainey, P.; Larkins, D. L. *Inorg. Chem.* **1998**, *37*, 2852.
(9) Darensbourg, D. J.; Rainey, P.; Yarbrough, J. C. *Inorg. Chem.* **2001**, *40*, 986.
(10) Cheng, M.; Darling, N. A.; Lobkovsky, E. B.; Coates, G. W. *Chem. Commun.* **2000**, 2007.
(11) Mang, S.; Cooper, A. I.; Colclough, M. E.; Chauhan, N.; Holmes, A. B. *Macromolecules* **2000**, *33*, 303.
(12) Darensbourg, D. J.; Wildeson, J. R.; Yarbrough, J. C.; Reibenspies, J. H. *J. Am. Chem. Soc.* **2000**, *122*, 12487.
(13) Burger, H.; Sawodny, W.; Wannaget, V. *J. Organomet. Chem.* **1965**, *3*, 113.
(14) *SMART 1000 CCD*; Bruker Analytical X-ray Systems: Madison, WI, 1999.
(15) *SAINT-Plus*, version 6.02; Bruker Analytical X-ray Systems: Madison, WI, 1999.
(16) Sheldrick, G. *SHELXS-86 Program for Crystal Structure Solution*; Institut fur Anorganische Chemie der Universitat: Gottingen, Germany, 1986.
(17) Sheldrick, G. *SHELXL-97 Program for Crystal Structure Refinement*; Institut fur Anorganische Chemie der Universitat: Gottingen, Germany, 1997.
(18) *SHELXTL*, version 5.0; Bruker Analytical X-ray Systems: Madison, WI, 1999.

Table 1. Crystallographic Data for Complexes **1a**, **1b**, **2a**, and **2b**

	1 − 4THF	**1a** − 4CH_3CN	**1b** − pyridine	**2**	**2a**
empirical formula	$C_{86}H_{62}F_{20}O_{28}Zn_7$	$C_{82}H_{48}F_{20}O_{22}N_6Zn_7$	$C_{29}H_{21}F_4O_4N_3Zn$·pyr	$C_{44}H_{44}Cl_8O_{12}Zn_2$	$C_{29}H_{21}Cl_4O_4N_3Zn$
fw	2380.94	2307.02	696.02	1179.24	682.72
cryst syst	monoclinic	triclinic	monoclinic	triclinic	monoclinic
space group	$P2(1)/n$	$P\bar{1}$	$P2(1)$	$P\bar{1}$	$P2(1)/c$
V, Å^3	4524(4)	2368.0(6)	1556.00(17)	4921.4(9)	2927(6)
Z	2	1	2	4	4
a, Å	15.145(7)	12.618(2)	11.6569(7)	10.8158(12)	14.688(17)
b, Å	14.852(7)	14.324(2)	10.9364(7)	12.6457(14)	9.213(10)
c, Å	20.147(9)	14.933(2)	12.8998(8)	36.794(4)	22.59(3)
α, deg		62.979(3)		88.179(2)	
β, deg	93.234(9)	84.892(3)	108.8850(10)	83.573(2)	106.76(2)
γ, deg		80.076(3)		79.803(2)	
T, K	110(2)	110(2)	110(2)	110(2)	110(2)
d(calcd), g/cm^3	1.748	1.442	1.537	1.602	1.549
abs coeff, mm^{-1}	1.945	1.852	0.862	1.468	1.244
R,[a] % [$I > 2\sigma(I)$]	6.42	6.47	2.56	9.44	7.71
R_w,[a] %	13.47	21.17	6.59	23.81	14.28

[a] $R = \sum||F_o| - |F_c||/\sum F_o$. $R_w = \{[\sum w(F_o^2 - F_c^2)^2/[\sum w(F_o^2)^2]\}^{1/2}$.

[s, {3,5-C_6H_3}]; 131.81, 132.59 [s, {ipso-C_6H_3}], 136.32, 139.31 [s, {2,6-C_6H_3}], 165.64, 172.46 [s, {−CO_2}].

Synthesis of [(2,6-Dimethoxybenzoate)$_{2x}$Zn$_x$](THF)$_y$ (3). A 10-mL THF solution of 2,6-dimethoxybenzoic acid (0.189 g, 1.04 mmol) was added to 5-mL THF solution of Zn[N($SiMe_3$)$_2$]$_2$ (0.20 g, 0.52 mmol), upon which a white solid, assumed to be an aggregate of bis-2,6-dimethoxybenzoate zinc, formed immediately. This precipitate was washed several times with hexanes and dried under vacuum to yield 0.218 (94%). IR(ν_{CO_2}): (KBr) 1643(m), 1597(s), 1547(s), 1425(s) cm^{-1}. ^{1}H NMR (d_6-DMSO): δ 1.75 [m, 4H {THF}], 3.60 [m, 4H {THF}], 3.71 [s, 12H {−OCH_3}], 6.60 [d, 4H {3,5-H}], 7.16 [t, 2H {4-H}]. ^{13}C{H} NMR (d_6-DMSO): δ 25.13 {THF}, 55.48 {−OCH_3}, 67.04 {THF}, 104.18 [s, {4-C_6H_3}]; 119.24 [s, {3,5-C_6H_3}]; 128.02 [s, {ipso-C_6H_3}], 155.58 [s, {2,6-C_6H_3}], 170.39 [s, {−CO_2}].

X-ray Crystallography. A Bausch and Lomb 10× microscope was used to identify suitable colorless crystals of **1**, **1a**, **1b**, **2**, and **2a** from a representative sample of crystals of the same habit. The representative crystal was coated in a cryogenic protectant (i.e., mineral oil, paratone, or apezeon grease) and was then fixed to a glass fiber, which in turn was fashioned to a copper mounting pin. The mounted crystals were then placed in a cold nitrogen stream (Oxford) maintained at 110 K on a Bruker SMART 1000 three circle goniometer.

Crystal data and details of data collection for the complexes are provided in Table 1. The X-ray data were collected on a Bruker CCD diffractometer and covered more than a hemisphere of reciprocal space by a combination of three sets of exposures; each exposure set had a different φ angle for the crystal orientation, and each exposure covered 0.3° in ω. The crystal-to-detector distance was 4.9 cm. Crystal decay was monitored by repeating the data collection for 50 initial frames at the end of the data set and analyzing the duplicate reflections; crystal decay was negligible. The space group was determined on the basis of systematic absences and intensity statistics.[14]

The structures were solved by direct methods. Full-matrix least-squares anisotropic refinement for all non-hydrogen atoms yielded R(F) and wR(F^2) values as indicated in Table 1 at convergence. Hydrogen atoms were place in idealized positions with isotropic thermal parameters fixed at 1.2 or 1.5 times the value of the attached atom. Neutral atom scattering factors and anomalous scattering factors were taken from the International Tables for X-ray Crystallography Vol. C.

The following software was used for the title compound: data reduction, SAINTPLUS (Bruker[15]); program(s) used to solve the structure, SHELXS-96 (Sheldrick[16]); program(s) used to refine the structure, SHELXL-97 (Sheldrick[17]); program(s) used for molecular graphics, SHELXTL version 5.0 (Bruker[18]); software used to prepare material for publication, SHELXTL version 5.0 (Bruker[18]).

High-Pressure Copolymerization of CO_2 with Cyclohexene Oxide. A sample of the active catalyst (0.100 g) was dissolved in 20.0 mL of cyclohexene oxide. The solution was loaded via an injection port into a 300 mL stainless steel Parr autoclave, which had previously been dried overnight under vacuum at 80 °C. The reactor was pressurized to 600 psi with CO_2 and heated to 80 °C, which increased the pressure to 750−800 psi. After 24−48 h of reaction time, the reactor was cooled and opened and the viscous/solid mixture isolated by dissolution in CH_2Cl_2 and precipitated out in MeOH. The polymer was analyzed by ^{1}H and ^{13}C NMR spectroscopy.

High-Pressure Copolymerization of CO_2 with Propylene Oxide. A 0.100 g amount of active catalyst was dissolved in 20.0 mL of propylene oxide. The resulting solution was added through the injection port to a predried 300 mL autoclave, and the reactor was pressurized to 600 psi with CO_2. The reactor was heated at 55 °C, raising the pressure to 650−700 psi, for 48 h. After this period of time, the reaction mixture was diluted with CH_2Cl_2 (1:10) and analyzed by infrared spectroscopy in the ν(CO) region.

High-Pressure Terpolymerization of CO_2 with Propylene Oxide and Cyclohexene Oxide. A 0.100 g amount of active catalyst was dissolved in a solution composed of 10.0 mL (∼50 mol %) of cyclohexene oxide and 7.0 mL (∼50 mol %) of propylene oxide. The resulting solution was added through the injection port of a 300 mL predried autoclave, and the reactor was pressurized to 600 psi with CO_2. The reactor was then heated to 55 °C, raising the pressure to 650−700 psi, for between 24 and 48 h. After this period of time, the reactor was opened, and the viscous/solid mixture was dissolved in CH_2Cl_2 and precipitated out in MeOH. The polymer was analyzed by ^{1}H and ^{13}C NMR spectroscopy.

Results and Discussion

Synthesis and X-ray Structural Characterization of Zinc Benzoate Complexes. Several multicentered zinc benzoate derivatives have been synthesized and isolated in greater than 50% purified yields from the reaction of 2 equiv

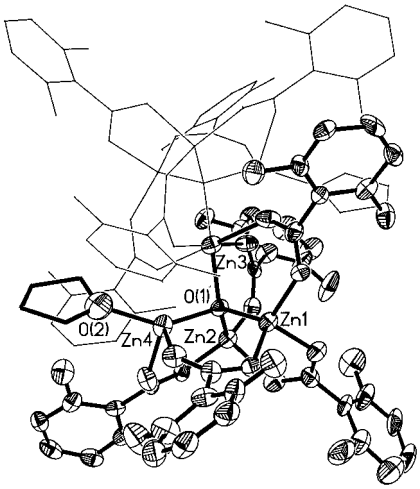

Figure 1. Thermal ellipsoid representation of the asymmetric unit of [(2,6-difluorobenzoate)$_{10}$O$_2$Zn$_7$](THF)$_2$, **1**, with the other half of the molecule shown as a stick drawing. Only the oxygen atom of the THF molecule was located and anisotropically refined.

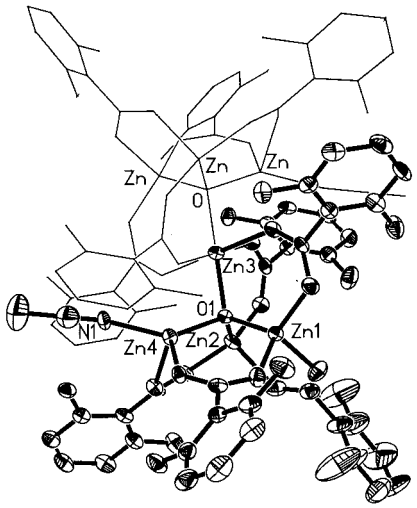

Figure 2. Thermal ellipsoid representation of the asymmetric unit of [(2,6-difluorobenzoate)$_{10}$O$_2$Zn$_7$](CH$_3$CN)$_2$, **1a**, with the other half of the molecule shown as a stick drawing.

of the respective benzoic acid and Zn[N(SiMe$_3$)$_2$]$_2$. For example, the reaction of 2,6-difluorobenzoic acid with Zn[N(SiMe$_3$)$_2$] in THF solution afforded complex **1**, [(2,6-difluorobenzoate)$_{10}$O$_2$Zn$_7$](THF)$_2$, in 77% yield. Crystals of **1** were obtained from a concentrated THF solution of the complex maintained at −20 °C. We have not specifically identified the source of oxide ligand. Presumably, it comes from water, for although the benzoic acid derivative was sublimed and stored under an inert atmosphere prior to its use, it is difficult to remove all traces of water from carboxylic acids. Upon vacuum-drying of complex **1**, the THF ligands are easily removed as indicated by C/H analysis and ^{1}H NMR spectroscopy. Recrystallization of complex **1** from acetonitrile results in X-ray quality crystals of the acetonitrile analogue of **1**, [(2,6-difluorobenzoate)$_{10}$O$_2$Zn$_7$](CH$_3$CN)$_2$, **1a**. However, dissolution of **1** in the stronger base pyridine led to aggregate disruption and formation of the mononuclear pyridine adduct, Zn(2,6-difluorobenzoate)$_2$(py)$_3$, **1b**.

Figures 1 and 2 display thermal ellipsoid drawings of **1** and **1a**, along with partial atom labeling schemes. Table 2 contains a compilation of selected bond distances and bond angles. The structures of complexes **1** and **1a** are nearly identical with the exception of the identity of the solvate molecules. These complexes are interesting seven zinc center aggregates where the metal atoms are interconnected by a combination of 10 bridging benzoate ligands and 2 μ_4-oxo ligands. The arrangement of the metal clusters is symmetrical through an inversion center at the central, octahedrally coordinated Zn(3) centers. The remaining three zinc atoms (Zn(1), Zn(2), and Zn(4)) are of tetrahedral geometry, along with their symmetry generated counterparts, and each share an oxo bridge to the central Zn(3) atom. This is best seen in the abbreviated representation of the Zn$_3$−μ_4O−Zn−μ_4OZn$_3$ core with bound THF molecules depicted in Figure 3. Two benzoate ligands are unsymmetrically bridged between the tetrahedrally coordinated Zn(1) and Zn(2) centers to Zn(3); that is, the corresponding Zn(1)−O and Zn(2)−O distances

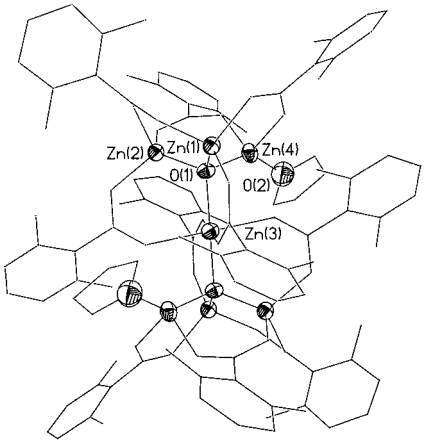

Figure 3. Abbreviated representation of the zinc−oxo core of complex **1**.

are 1.945(8) and 1.946(8) Å in **1** and 1.947(6) and 1.957(6) Å in **1a**, as compared to the significantly longer octahedrally coordinated Zn(3)−O distances of 2.207(8) and 2.164(8) Å in **1** and 2.184(6) and 2.167(6) Å in **1a**. The remaining three benzoate bridges are fairly symmetrically bonded to the zinc centers. The Zn−O$_{oxo}$ bond lengths cover a small range (1.919(7)−1.984(7) Å in **1** and 1.917(6)−1.987(5) Å in **1a**) with an average distance of 1.944 Å in **1** and 1.945 Å in **1a**. The bridging modes for all of the benzoate ligands were found to be in a *syn*−*syn* configuration. The tetrahedral arrangement of the bridged Zn(1)/Zn(2)/Zn(3)/Zn(4) atoms is similar to a four zinc centered complex previously reported by Straughan, as described in Figure 4.[19] However, instead of a benzoate bridge linking Zn(3) and Zn(4) together, thus satisfying their tetrahedral environs, a THF (**1**) or acetonitrile (**1a**) molecule is bound to Zn(4), leaving a trigonally coordinated Zn(3) foundation open to symmetrically incorporate Zn(1A)/Zn(2A)/Zn(4A) along with their benzoate and oxo bridging groups. The Zn(4)−O$_{THF}$ bond distance in complex **1** was found to be 2.035(10) Å, and the analogous

(19) Clegg, W.; Harbron, D.; Holman, C.; Hunt, P.; Little, I.; Straughan, B. *Inorg. Chim. Acta* **1991**, *186*, 51.

Table 2. Selected Bond Distances (Å) and Bond Angles (deg) for Complexes **1**, **1a**, **1b**, **2**, and **2a**[a]

	1	**1a**		**1**	**1a**
Zn(1)−O(1D)	1.979(8)	1.965(6)	O(1D)−Zn(1)−O(2C)	102.6(3)	99.2(3)
Zn(1)−O(2B)	1.945(8)	1.947(6)	O(2C)−Zn(1)−O(1)	112.6(3)	114.1(3)
Zn(1)−O(2C)	1.977(8)	1.973(7)	O(1)−Zn(2)−O(1C)	108.3(3)	109.7(3)
Zn(1)−O(1)	1.919(7)	1.917(6)	O(1)−Zn(2)−O(1A)	115.1(3)	113.2(2)
Zn(2)−O(1A)	1.946(8)	1.957(6)	O(1)−Zn(2)−O(1E)	119.9(3)	117.0(3)
Zn(2)−O(1C)	1.995(8)	1.993(7)	O(1E)−Zn(2)−O(1A)	108.2(3)	115.7(3)
Zn(2)−O(1E)	1.941(8)	1.945(6)	O(1E)−Zn(2)−O(1C)	102.8(3)	99.6(3)
Zn(2)−O(1)	1.927(7)	1.932(6)	O(1A)−Zn(2)−O(1C)	99.9(3)	98.7(3)
Zn(3)−O(2A)	2.164(8)	2.167(6)	O(1)−Zn(3)−O(2A)	98.1(3)	100.4(2)
Zn(3)−O(1B)	2.207(8)	2.184(6)	O(1)−Zn(3)−O(1B)	97.3(3)	97.9(2)
Zn(3)−O(1)	1.984(7)	1.987(5)	O(1B)−Zn(3)−O(2A)	93.7(3)	90.6(2)
Zn(4)−O(2D)	1.966(7)	1.996(6)	O(2D)−Zn(4)−O(2)	105.9(4)	
Zn(4)−O(2E)	2.053(9)	2.071(6)	O(2E)−Zn(4)−O(2)	91.9(4)	
Zn(4)−O(1)	1.946(8)	1.944(6)	O(1)−Zn(4)−O(2)	139.8(4)	
Zn(4)−O(2)	2.035(10)		O(2D)−Zn(4)−N(1)		104.0(3)
Zn(4)−N(1)		2.028(8)	O(2E)−Zn(4)−N(1)		89.2(3)
Zn(1)−O(1)−Zn(2)	107.7(4)	107.6(3)	O(1)−Zn(4)−N(1)		140.1(3)
Zn(1)−O(1)−Zn(3)	115.2(4)	115.3(3)	O(2D)−Zn(4)−O(2E)	99.9(3)	98.4(3)
Zn(1)−O(1)−Zn(4)	109.7(3)	110.3(3)	O(1)−Zn(4)−O(2E)	102.8(3)	100.6(2)
Zn(2)−O(1)−Zn(3)	111.7(3)	109.9(3)	O(1)−Zn(4)−O(2D)	108.0(3)	112.5(2)
Zn(2)−O(1)−Zn(4)	108.5(4)	110.6(3)	O(2E)−C(1E)−O(1E)	126.6(12)	125.3(9)
Zn(3)−O(1)−Zn(4)	103.9(3)	103.1(3)	O(2D)−C(1D)−O(1D)	127.3(11)	128.2(8)
O(1D)−Zn(1)−O(2B)	106.6(3)	105.8(3)	O(2B)−C(1B)−O(1B)	125.8(12)	127.4(9)
O(2B)−Zn(1)−O(1)	118.2(3)	117.9(3)	O(2A)−C(1A)−O(1A)	124.5(11)	125.4(8)
O(1D)−Zn(1)−O(1)	112.8(3)	109.8(3)	O(2C)−C(1C)−O(1C)	124.9(12)	126.0(9)
O(2B)−Zn(1)−O(2C)	102.4(3)	108.1(3)			

Complex **1b**

Zn(1)−O(3)	2.024(2)	O(1)−Zn(1)−O(3)	128.46(8)
Zn(1)−O(1)	2.036(2)	O(1)−Zn(1)−N(1)	88.64(10)
Zn(1)−N(1)	2.177(3)	O(1)−Zn(1)−N(2)	134.85(10)
Zn(1)−N(2)	2.1135(18)	O(1)−Zn(1)−N(3)	89.44(10)
Zn(1)−N(3)	2.195(3)	N(1)−Zn(1)−N(3)	177.98(10)

Complex **2**

Zn(1)−O(2A)	1.941(5)	O(2A)−Zn(1)−O(7A)	108.9(2)
Zn(1)−O(3A)	1.957(5)	O(3A)−Zn(1)−O(5A)	109.8(2)
Zn(1)−O(5A)	1.942(6)	O(3A)−Zn(1)−O(7A)	119.6(2)
Zn(1)−O(7A)	1.950(6)	O(5A)−Zn(1)−O(7A)	109.6(2)
Zn(2)−O(4A)	2.007(5)	O(4A)−Zn(1)−O(6A)	98.1(2)
Zn(2)−O(6A)	2.072(5)	O(4A)−Zn(1)−O(8A)	103.7(2)
Zn(2)−O(8A)	2.040(5)	O(4A)−Zn(1)−O(9A)	166.2(2)
Zn(2)−O(9A)	2.095(6)	O(4A)−Zn(1)−O(10A)	84.6(2)
Zn(2)−O(10A)	2.169(5)	O(4A)−Zn(1)−O(11A)	84.0(2)
Zn(2)−O(11A)	2.165(5)	O(3A)−C(8A)−O(4A)	127.1(6)
O(2A)−Zn(1)−O(3A)	93.1(2)	O(5A)−C(15A)−O(6A)	127.6(7)
O(2A)−Zn(1)−O(5A)	114.9(2)	O(7A)−C(22A)−O(8A)	126.6(7)

Complex **2a**

Zn(1)−O(1)	1.977(11)	O(1)−Zn(1)−O(4)	121.0(4)
Zn(1)−O(3)	2.183(11)	O(3)−Zn(1)−N(1)	91.6(5)
Zn(1)−O(4)	2.348(10)	O(3)−Zn(1)−N(2)	91.7(4)
Zn(1)−N(1)	2.108(12)	O(3)−Zn(1)−N(3)	89.4(5)
Zn(1)−N(2)	2.087(11)	N(1)−Zn(1)−N(3)	157.8(5)
Zn(1)−N(3)	2.100(13)	O(1)−Zn(1)−N(2)	90.1(5)
O(1)−Zn(1)−O(3)	176.3(4)	N(2)−Zn(1)−N(1)	95.3(5)

[a] Estimated deviations are given in parentheses.

$Zn(4)-N_{acetonitrile}$ bond distance in **1a** was determined to be 2.028(8) Å. In addition to the two THF or acetonitrile molecules bound to Zn(4) and Zn(4A) in complexes **1** and **1a**, four additional molecules of each respective solvent were found in the crystal lattices.

A thermal ellipsoid rendering of the pyridine complex (**1b**) derived from the dissolution of complex **1** in pyridine can be seen in Figure 5, with selected bond distances and bond angles listed in Table 2. The structure of **1b** consists of a distorted trigonal bipyrimidal arrangement of three pyridine and two benzoate ligands about the zinc center. The benzoate ligands are bound essentially in an unidentate fashion to zinc, where the Zn−O(1) and Zn−O(3) bond distances are 2.036(2) and 2.024(2) Å, with the distal oxygens (O(2) and O(4)) being 2.796 and 2.953 Å from the zinc center, respectively. The two axial Zn−N bond lengths were found to be slightly longer than the Zn−N equatorial bond distance, with the average $Zn-N_{ax} = 2.186[3]$ Å and the $Zn-N_{eq} = 2.1135(18)$ Å. The two axial pyridine ligands form a N(1)−Zn−N(3) bond angle of 177.98(10)° and an average bond angle of 91.33° between the ligands in the trigonal plane. The remaining pyridine ligand in the metal's coordination sphere forms a trigonal plane with the benzoate groups affording an average N(2)−Zn−O bond angle of

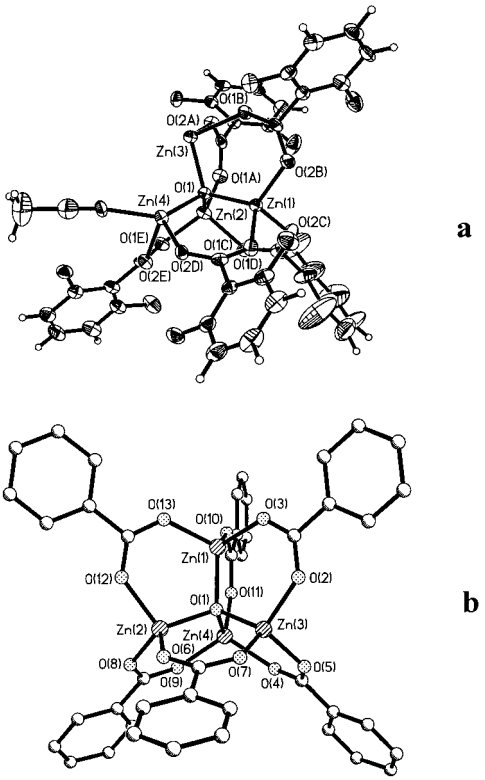

Figure 4. (a) Thermal ellipsoid representation of the independently defined portion of complex **1a**. (b) [(Benzoate)$_6$OZn] complex reported by Straughan in ref 19.

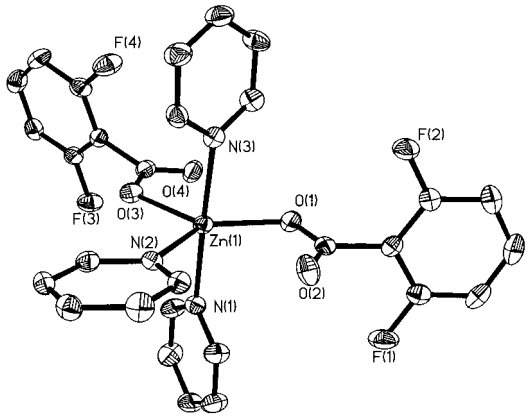

Figure 5. Thermal ellipsoid representation of [(2,6-difluorobenzoate)$_2$Zn-(NC$_5$H$_5$)$_3$], **1b**.

115.77[10]°. A fourth pyridine molecule was found in the crystal lattice of **1b**. The O(1)−Zn−O(3) bond angle of 128.46(8)° exists between the benzoate groups.

By way of contrast to the process described previously leading to formation of complex **1**, the reaction of Zn-[N(SiMe$_3$)$_2$]$_2$ with 2,6-dichlorobenzoate in THF has led to a more anticipated product devoid of μ-oxo ligands. That is, the reaction affords the dimeric complex, [(2,6-dichlorobenzoate)$_4$Zn$_2$](THF)$_3$ (**2**). A thermal ellipsoid representation of complex **2** is shown in Figure 6 for one of the independently generated molecules in the unit cell. Selected bond distances and bond angles may be found in Table 2. The two zinc centers are unsymmetrically bridged by three benzoate ligands. Interestingly, one zinc center possesses a

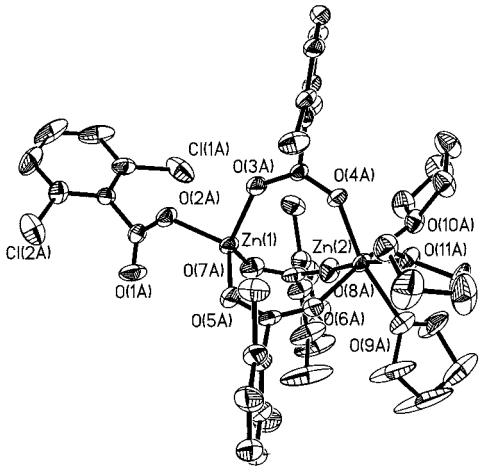

Figure 6. Thermal ellipsoid representation of [(2,6-dichlorobenzoate)$_4$Zn$_2$]-(THF)$_3$, **2**.

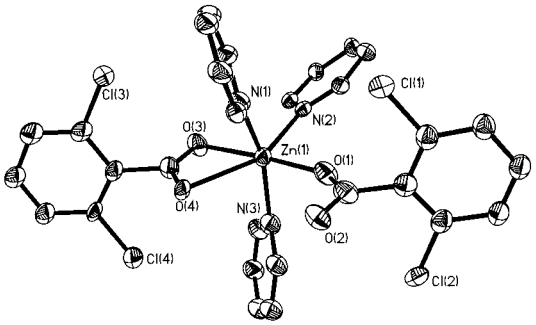

Figure 7. Thermal ellipsoid representation of [(2,6-dichlorobenzoate)$_2$Zn-(NC$_5$H$_5$)$_3$], **2a**.

distorted tetrahedral ligand environment, where the fourth ligand is a unidentate benzoate group (distal O(1A)···Zn(1) separation = 3.225 Å). The second zinc center has an octahedral arrangement of ligands which is accomplished by the additional binding of three THF molecules. The average Zn−O bond distance for the tetrahedral zinc was found to be 1.948[5] Å, with an average O−Zn−O bond angle of 109.36°. For the octahedral environment, the average Zn−O bond distance was determined to be 2.040[5] Å for the bridging benzoates and 2.143[5] Å for the THF linkage.

Analogous to the behavior of complex **1** upon dissolution in pyridine, complex **2** afforded X-ray quality crystals of Zn(2,6-dichlorobenzoate)$_2$(py)$_3$ (**2a**), which results from disruption of the zinc dimer by the strongly coordinating pyridine ligand. A thermal ellipsoid representation of complex **2a** is shown in Figure 7, and selected bond distances and bond angles may be found in Table 2. The structure of **2a** closely resembles that of its difluorobenzoate analogue, complex **1b**. That is, complex **2a** consists of a distorted trigonal bipyrimidal arrangement of three pyridine and two benzoate ligands around a common zinc center. However, in this instance, possibly because of the stronger binding ability of the chlorobenzoate ligand relative to its fluoro counterpart, one of the benzoate ligands is unsymmetrically bound in a bidentate fashion with the Zn−O(3) bond distance at 2.183(11) Å being significantly shorter than the Zn−O(4) bond length of 2.348(10) Å. This change in binding mode distorts the axial N(1)−Zn−N(3) bond angle to 157.8(5)°

Table 3. Catalytic Activity for the Copolymerization of Carbon Dioxide and Cyclohexene Oxide[a]

catalyst	turnover number (g·poly/g·Zn)	turnover frequency (g·poly/g·Zn/hr)
$[Zn_7(O_2C\text{-}2,6\text{-}F_2C_6H_3)_{10}O_2](THF)_2$, **1**	494	10.3
$[Zn_2(O_2C\text{-}2,6\text{-}Cl_2C_6H_3)_4](THF)_3$, **2**	874	16.7
$[Zn(O_2C\text{-}2,6\text{-}(OMe)_2C_6H_2)_2]_n(THF)_m$, **3**	329	7.2

[a] Catalyst loading (0.100 g), 20.0 mL of cyclohexene oxide, CO_2 at ambient temperature 41.3 bar. Reaction conditions: 80 °C at a total pressure of 55 bar.

as compared to the nearly linear angle (177.98(10)°) seen in **1b**. Concomitantly, the O(1)−Zn−O(3) bond angle of 176.3(4)° is more obtuse than its corresponding value of 128.46(8)° in complex **1b**. Hence, the geometry of complex **2a** might be better described as a highly distorted octahedral structure.

Note. Average esd's are provided in [ ], whereas ( ) are used for a single esd value.

Reactivity Studies of Zinc Benzoate Derivatives for the Copolymerization of Carbon Dioxide and Epoxides. The infrared spectra of the zinc benzoate complexes **1** and **2** in the $\nu(CO_2)$ region recorded in both the solid state (KBr) and solution (THF) were shown to be quite similar (see Experimental Section). These observations are suggestive of the solution structures of **1** and **2** at ambient temperature strongly resembling their well-defined solid-state structures. Hence, it is highly likely that upon dissolution of these derivatives in epoxides a similar solution structure is present, with epoxide ligands occupying the zinc sites previously occupied by THF molecules. Because various *nonstructurally characterized* zinc carboxylates have been demonstrated to be quite effective as catalysts for the copolymerization of CO_2 and epoxides, it was naturally of interest to examine the activity of these structurally characterized species. That is, the soluble, nonstructurally characterized zinc monoesters of maleic acid[3,4] and zinc crotonate catalyst systems[5] have shown high activity for the copolymerization of CO_2 and cyclohexene oxide to afford alternating copolymer with little to no polyether linkages (eq 1). Of course, the heterogeneous zinc glutarate catalyst has received much academic and industrial attention for this process.[2,20,21]

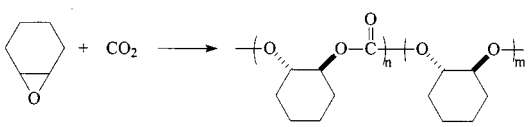

(1)

Complexes **1**−**3** have been tested for their ability to catalyze the copolymerization of cyclohexene oxide and carbon dioxide to provide high molecular weight poly(cyclohexenylene carbonate). These catalysts exhibit activities which are compiled in Table 3 which are very close to those seen in the related soluble zinc carboxylates previously reported in the literature.[3−5] It is likely that in all of these systems a similar zinc species is responsible for the catalysis of the process depicted in eq 1. Whether the metal species is a zinc aggregate complex or some species produced by degradation of a zinc aggregate is not definitively known. Although complex **1** can be recovered from a refluxing THF solution maintaining its original solid-state structure, there may be significant rearrangement or disruption of all or part of this structure during the copolymerization process. Similar to recently developed zinc phenoxide catalysts containing fluorine substituents,[10] complexes **1**−**3** are stable in moist air and do not lose activity when allowed to stand in a moist oxygen atmosphere for prolonged periods of time. In addition, it is particularly notable that the polymers produced have essentially 100% carbonate linkages, which is characteristic of polymer produced by zinc catalysts with one site for epoxide binding. The percentage of carbonate linkages is assessed from the integration of the methine protons of the carbonate linkages ($\delta = 4.60$ ppm) and the ether linkages ($\delta = 3.45$ ppm). A short while ago, Scott and co-workers developed a series of similar zinc cluster catalysts by reacting diethyl zinc with tris(3,5-dialkyl-2-hydroxyphenyl) methane.[22] Although these complexes are structurally interesting, they displayed reduced activities (1.33−2.54 g poly/g Zn·hr) and inadequate control over CO_2 incorporation (60−80% carbonate linkages).

The terpolymerization of propylene oxide (50 mol %), cyclohexene oxide (50 mol %), and CO_2, employing catalyst **2**, the most active catalyst for the copolymerization of cyclohexene oxide and CO_2, exhibited an average turnover number of 523 g poly/g Zn and a turnover frequency of 10.88 g poly/g Zn/hr. The polymer produced has 88.15 mol % cyclohexene oxide carbonate linkages, 6.44 mol % propylene carbonate linkages, and 5.41 mol % propylene ether linkages. Propylene carbonate and ether linkages show up in the ^1H NMR spectrum at 5.01 and 3.59 ppm, respectively. Interestingly, as with the dimeric zinc phenoxide systems, there are no cyclohexene oxide ether linkages in the terpolymer. On the other hand, the copolymerization of propylene oxide and CO_2, using **2** as catalyst, produced only a thin film of polymer. A comparison of cyclic carbonates to polycarbonates produced was determined by infrared spectroscopy, with propylene polycarbonate showing a $\nu(CO_2)$ absorption at 1750 cm^{-1} and cyclic propylene carbonate exhibiting a $\nu(CO_2)$ mode at 1800 cm^{-1}. Under similar reaction conditions to those used in cyclohexene oxide/CO_2 copolymerization, propylene cyclic carbonate is the major product produced. Upon lowering the reaction temperature to 40 °C, propylene polycarbonate dominates over the cyclic carbonate as previously noted.[23]

Summary

Herein, we have reported on the synthesis and structural characterization of several zinc carboxylates, derivatives which are closely related to nonstructurally defined hetero-

(20) Ree, M.; Bae, J. Y.; Jung, J. H.; Shin, T. J. *J. Polym. Sci., Part A: Polym. Chem.* **1999**, *37*, 1863.
(21) (a) Rokicki, A. U.S. Patent No. 4, 943, 677, July 24, 1990. (b) PAC Polymers Inc., Newark, DE.
(22) Dinger, M.; Scott, M. *Inorg. Chem.* **2001**, *40*, 1029.
(23) Darensbourg, D. J.; Holtcamp, M. W.; Struck, G. E.; Zimmer, M. S.; Niezgoda, S. A.; Rainey, P.; Robertson, J. B.; Draper, J. D.; Reibenspies, J. H. *J. Am. Chem. Soc.* **1999**, *121*, 107.

geneous and homogeneous zinc carboxylates which serve as catalyst precursors for the copolymerization of CO_2 and epoxide to provide polycarbonates. Although these complexes exist as monomeric species when dissolved in strong bases such as pyridine, they are dimeric or multinuclear derivatives in the presence of less coordinating bases such as THF or acetonitrile. In particular, the acetonitrile and THF adducts of **1** exist as seven zinc membered clusters, where the metal centers are linked together by *syn*−*syn* μ-benzoate and μ_4-oxo bridges. Solution and solid-state infrared spectroscopy in the ν_{CO_2} region demonstrates that these derivatives remain intact upon dissolution in THF and suggests a similar behavior when dissolved in epoxides. The perception that the catalytically active zinc species remains an aggregate or dimer is reinforced by the presence of greater than 99% carbonate linkages in the resulting polymer. That is, if complexes **1**−**3** were rendered monomeric in the epoxide solution during the polymerization process, this degree of CO_2 incorporation would be highly unlikely because of multiple open binding sites for the epoxide coordination and consequent formation of ether linkages.[10] Nevertheless, it should be reiterated here that there may be significant rearrangement of the solid-state structures during the copolymerization process. These complexes, although found to be active for the copolymerization of cyclohexene oxide and CO_2 along with the terpolymerization of cyclohexene oxide/propylene oxide/CO_2, did not fulfill our goal to develop effective catalysts for propylene oxide/CO_2 copolymerization. On the surface, this observation would appear to discredit the Kuran hypothesis that multinuclear zinc complexes should lead to reduced cyclic carbonate formation with concomitant polycarbonate production.[6] However, even if the assumption that these zinc aggregates remain intact during polymerization is true, the systems studied herein and elsewhere do not possess readily accessible coordination sites on adjacent zinc centers, a requirement which is essential for inhibiting the back biting reaction.

Finally, the quite similar catalytic behavior and activity for the copolymerization of CO_2 and cyclohexene oxide exhibited by these structurally defined zinc carboxylates as compared to the less well-defined homogeneous catalysts currently in the literature suggest a close relationship between the nature of the active zinc species in all of these catalytic systems.

Acknowledgment. Financial support from the National Science Foundation (CHE-99-10342 and CHE 98-07975 for the purchase of X-ray equipment) and the Robert A. Welch Foundation is greatly appreciated.

Supporting Information Available: Complete details (CIF format) of the X-ray diffraction studies on **1**, **1a**, **1b**, **2**, and **2a**. This material is available free of charge via the Internet at http://pubs.acs.org.

IC0107983